

Dynamical Mean Field Theory of Optical Third Harmonic Generation

S. Akbar JAFARI^{1,2*}, Takami TOHYAMA¹ and Sadamichi MAEKAWA^{1,3}

¹*Institute for Materials Research, Tohoku University, Sendai 980-8577*

²*Department of Physics, Isfahan University of Technology, Isfahan 84156, Iran*

³*CREST, Japan Science and Technology Agency, Kawaguchi, Saitama 332-0012*

(Received April 26, 2006; accepted June 27, 2006; published August 10, 2006)

We formulate the third harmonic generation (THG) within the dynamical mean field theory (DMFT) approximation of the Hubbard model. In the limit of large dimensions, where DMFT becomes exact, the vertex corrections to current vertices are identically zero. Hence, the calculation of the THG spectrum reduces to a time-ordered convolution, followed by an appropriate analytic continuation. We present a typical THG spectrum of the Hubbard model obtained by this method. Within our DMFT calculation, we observe a nontrivial approximate *scaling* function describing the THG spectra in all Mott insulators, independent of the gap magnitude.

KEYWORDS: third harmonic generation, Mott insulator, dynamical mean field

DOI: [10.1143/JPSJ.75.083706](https://doi.org/10.1143/JPSJ.75.083706)

Nonlinear optical interactions of laser fields with matter provide powerful spectroscopic tools for the understanding of microscopic processes. The ability to control pulse durations (to a few femtoseconds), bandwidths (up to 1 Hz resolution), and peak intensities (up to 10^{19} W/cm²) provides novel methods of investigation for elementary dynamic events occurring in matter.¹⁾

Observation of a large third order nonlinear susceptibility in a quasi 1D Mott insulator Sr₂CuO₃ ($\chi^{(3)}$ values in the range 10^{-8} to 10^{-5} e.s.u.)^{4,5)} poses the problem of nonlinear optical response in correlated insulators.

In systems with large on-site Coulomb interactions, the 1D system has the largest optical nonlinearity because of the decoupling of spin and charge degrees of freedom.^{6,7)} On the other hand, mean field analysis shows that among SDW-ordered systems, the largest third order optical response appears in 2D.³⁾ However, a mean field treatment of this manner does not address the Mott insulators considered in the experiments of ref. 4. Therefore, we employ the dynamical mean field theory (DMFT) approximation to formulate the nonlinear optical response of the Mott insulators.

DMFT approximation becomes exact in $d \rightarrow \infty$. In this limit, the self-energy becomes a purely local quantity determined by the self-consistent Anderson model. Then, the matrix elements determining spectral weights are encoded in the local self-energy. In this limit, the matrix element summations reduce to density of states (DOS) integrations. Therefore, the combined DOS and self-energy effects gives rise to the nonlinear optical response of the system.

We formulate a nonlinear response theory, for THG within the DMFT approximation and propose a numerically feasible method to avoid expensive computations. To the best of our knowledge, this is the first application of DMFT to nonlinear optics.

The general THG lineshape within the DMFT framework occurs as a strong peak in three-photon resonance, followed by a shoulder in two-photon resonance, and a very weak feature in one-photon resonance. If we scale the frequencies

with the gap magnitude, the three-photon contributions obtained for various on-site Coulomb repulsion, fall approximately on the same curve. This approximate behavior in Mott insulators becomes exact in single-particle insulators.³⁾

We start with the Hubbard model at half filling

$$H = \frac{\tilde{t}}{\sqrt{d}} \sum_{\langle i,j \rangle, s} (c_{is}^\dagger c_{js} + \text{h.c.}) + U \sum_j \left(n_{j\uparrow} - \frac{1}{2} \right) \left(n_{j\downarrow} - \frac{1}{2} \right), \quad (1)$$

where c_{is}^\dagger creates an electron at site i with spin $s = \uparrow, \downarrow$. The dimension of the lattice is d . Here, the $1/\sqrt{d}$ scaling of the hopping term ensures that the average kinetic energy per particle in the limit $d \rightarrow \infty$ remains finite.⁸⁾

If we now imagine that we integrate out all degrees of freedom on various lattice sites, except for the one at the origin, we obtain the following effective action for this “impurity” site:

$$S_{\text{eff}} = - \int_0^\beta \int_0^\beta d\tau d\tau' \sum_\sigma c_{o\sigma}^\dagger(\tau) \mathcal{G}_0^{-1}(\tau - \tau') c_{o\sigma}(\tau') + U \int_0^\beta n_{o\uparrow}(\tau) n_{o\downarrow}(\tau). \quad (2)$$

Here, the impurity propagator $\mathcal{G}_0(\tau - \tau')$ describes temporal quantum fluctuations between the four possible states of a single site at the origin, which must be determined self-consistently.

The simplest way to solve an effective impurity problem of this type is by the second order perturbation, which gives

$$\Sigma(\tau) = \frac{U^2}{4} \mathcal{G}_0(\tau) \mathcal{G}_0(\tau) \mathcal{G}_0(-\tau). \quad (3)$$

This gives the lattice Green’s function as

$$G(\mathbf{k}, i\omega_n) = 1/(i\omega_n - \varepsilon_{\mathbf{k}} - \Sigma(i\omega_n)). \quad (4)$$

The projection of this function on site “o” is given by

$$G(i\omega_n) = \int \frac{D(\varepsilon) d\varepsilon}{i\omega_n - \varepsilon - \Sigma(i\omega_n)}, \quad (5)$$

*E-mail: akbar@imr.tohoku.ac.jp

where $D(\varepsilon)$ is the lattice density of states. Finally, the self-consistency between the lattice (G) and impurity (\mathcal{G}_0) is given by the Dyson equation

$$\mathcal{G}_0^{-1}(i\omega_n) = \Sigma(i\omega_n) + G^{-1}(i\omega_n), \quad (6)$$

which is used to update \mathcal{G}_0 if the consistency was not achieved.⁸⁾

Solving the set of eqs. (3), (5), and (6) for various values of Hubbard U , captures the physics of a Mott metal-to-insulator transition.⁹⁾ The essential many-body quantity obtained by solving the local impurity problem is the self-energy, which encodes the matrix element effects, as will be shown in the following. We solve¹⁰⁾ the above set of equations at zero temperature for a Bethe lattice DOS of type $D(\varepsilon) = \frac{2}{\pi} \sqrt{1 - \varepsilon^2}$, which corresponds to renormalized hopping $\tilde{t} = t\sqrt{d} = 1/2$.

The third order nonlinear optical response per unit volume is related to the four-current correlation $\chi_{jj}^{(3)}(\omega; \omega_1, \omega_2, \omega_3)$ by¹¹⁾

$$\chi^{(3)}(\omega; \omega_1, \omega_2, \omega_3) = \frac{1}{3!} \left(\frac{-i}{\hbar} \right)^3 \frac{1}{V} \frac{\chi_{jj}^{(3)}(\omega; \omega_1, \omega_2, \omega_3)}{i\omega_\sigma \omega_1 \omega_2 \omega_3}, \quad (7)$$

where $\omega = -\omega_\sigma = -(\omega_1 + \omega_2 + \omega_3)$, and the four-current correlation function is given by

$$\begin{aligned} \chi_{jj}^{(3)}(\omega; \omega_1, \omega_2, \omega_3) = & \int dx dx_1 dx_2 dx_3 e^{i(\omega t + \omega_1 t_1 + \omega_2 t_2 + \omega_3 t_3)} \\ & \times \langle T_c j(x) j(x_1) j(x_2) j(x_3) \rangle, \end{aligned}$$

where $j(x)$ is the current operator in space-time $x = (r, t)$. Here, T_c denotes the time-ordering of the Keldysh path.¹²⁾ Although the general formulation can be expressed in terms of Keldysh Green's functions, for parametric processes,²⁾ i.e., processes in which final and initial states are identical, in practice one can avoid the use of Keldysh Green's functions. In such a case, one can use an ordinary Green's function to calculate the *time ordered* diagrams, followed

by appropriate analytic continuation to ensure the correct $\nu + i\eta$ behavior of the fully retarded optical responses.³⁾

The case of third harmonic generation corresponds to $\omega_1 = \omega_2 = \omega_3 = \nu$ such that we have

$$\chi^{\text{THG}}(\nu) \equiv \chi^{(3)}(-3\nu; \nu, \nu, \nu) = \frac{1}{18} \left(\frac{1}{\hbar} \right)^3 \frac{\langle JJJJ \rangle^{\text{THG}}(\nu)}{\nu^4}, \quad (8)$$

$$\langle JJJJ \rangle^{\text{THG}}(\nu) = \int dx e^{-3i\nu t} \Pi_i dx_i e^{i\nu t_i} \langle T j(t) j(x_1) j(x_2) j(x_3) \rangle.$$

The Feynman diagram corresponding to the THG process¹³⁾ is shown in Fig. 1. In the limit of infinite dimensions, vertex corrections to odd parity operators identically vanish by Ward identity. To verify this, we express the Ward identity as¹⁴⁾

$$-ik_\mu \Gamma^\mu(p+k, k) = G^{-1}(p+k) - G^{-1}(k), \quad (9)$$

where the summation over $\mu = 0, 1, \dots, d$ is understood and p, k are $(d+1)$ -vectors. Using the Dyson equation, the right-hand side becomes $\Sigma(k+p) - \Sigma(k)$. In the $d \rightarrow \infty$ limit, self-energy is purely local⁸⁾ (no k dependence), and hence it vanishes. Now, since the current (\propto velocity) vertex has odd parity under $\mathbf{k} \rightarrow -\mathbf{k}$, the vertex correction Γ^μ identically vanishes.

Therefore, the four-current correlation $\langle JJJJ \rangle^{\text{THG}}(\nu)$ in

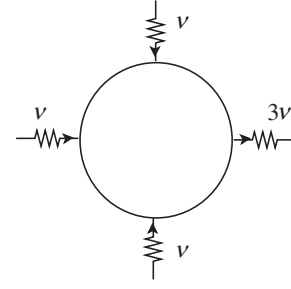


Fig. 1. Feynman diagram corresponding to the third harmonic generation. This diagram represents the *time-ordered* four-current correlation. To obtain the *fully retarded* four-current correlation, we ensure the correct $\nu + i\eta$ analytic behavior.

Fig. 1 can be obtained by simple convolution. The Green's functions over the loop are self-consistent lattice Green's functions obtained from the impurity solver by iterated perturbation theory.⁸⁾ Now, let us further simplify $\langle JJJJ \rangle^{\text{THG}}(\nu)$ in the $d \rightarrow \infty$ limit. Equation (8) can be written as

$$\begin{aligned} \chi^{\text{THG}}(i\nu) = & \frac{1}{18} \frac{\langle J_1 J_1 J_1 J_1 \rangle}{\nu^4} = \frac{8\tilde{t}^4}{9\nu^4} \frac{1}{Nd\beta} \sum_{\mathbf{k}, \omega_n} \sin^4(k_1) \\ & \times G_{k\sigma}(i\omega_n) G_{k\sigma}(i\omega_n + i\nu) G_{k\sigma}(i\omega_n + 2i\nu) G_{k\sigma}(i\omega_n + 3i\nu), \end{aligned}$$

where we have used the fact that the current vertex in direction no. 1 is $2\tilde{t} \sin(k_1)$. To proceed further, we need to define $\rho_0(\varepsilon) = \frac{1}{Nd} \sum_{\mathbf{k}} \sin^4(k_1) \delta(\varepsilon - \varepsilon_{\mathbf{k}})$. To take the limit $d \rightarrow \infty$, we Fourier transform $\rho_0(\varepsilon)$ as

$$\begin{aligned} \rho_0(s) = & \int \rho_0(\varepsilon) e^{is\varepsilon} d\varepsilon = \frac{1}{Nd} \sum_{\mathbf{k}} \sin^4 k_1 e^{is\varepsilon_{\mathbf{k}}} \\ = & \left[\int_{-\pi}^{\pi} e^{-2ist \cos k} \frac{dk}{2\pi} \right]^{d-1} \left[\int_{-\pi}^{\pi} \sin^4 k_1 e^{-2ist \cos k_1} \frac{dk_1}{2\pi} \right] \\ = & [J_0(2st)]^{d-1} \times \frac{1}{8} [3J_0(2st) - 4J_2(2st) + J_4(2st)] \\ = & \frac{1}{8} \left[3[J_0(2st)]^d + \mathcal{O}\left(\frac{1}{d}\right) \right], \end{aligned}$$

where J_n is a Bessel function of order n . In the last line we have used the fact that the hopping matrix element scales like $t = \tilde{t}/\sqrt{d}$ for $d \rightarrow \infty$; hence, $st \ll 1$. Thus, we can ignore J_2 and J_4 as compared to J_0 by using $J_n(x) \approx x^n/(2^n n!)$. Repeating the above algebra without $\sin^4 k_1$ shows that, $[J_0(2st)]^d$ is indeed the Fourier transform of $D(\varepsilon)$. Therefore,

$$\rho_0(\varepsilon) = \frac{3}{8} D(\varepsilon), \quad (10)$$

which allows us to write

$$\begin{aligned} \chi^{\text{THG}}(i\nu) = & \frac{\tilde{t}^4}{3\nu^4\beta} \sum_{\omega_n} \int d\varepsilon D(\varepsilon) \\ & \times G(\varepsilon, i\omega_n) G(\varepsilon, i\omega_n + i\nu) G(\varepsilon, i\omega_n + 2i\nu) G(\varepsilon, i\omega_n + 3i\nu). \end{aligned} \quad (11)$$

We see that in $d \rightarrow \infty$, the \mathbf{k} summation simply becomes a DOS integration. In the following ε stands for $\varepsilon_{\mathbf{k}}$, and the explicit ε subscript emphasizes the \mathbf{k} label. This derivation indicates that the other four current correlations like $\langle J_1 J_1 J_2 J_2 \rangle$ in the $d \rightarrow \infty$ limit differ from $\langle J_1 J_1 J_1 J_1 \rangle$ by a

numerical factor. Therefore THG in the limit of $d \rightarrow \infty$ is independent of various directions in space. Hence, DMFT can not distinguish optical spectroscopies with polarized light from those with unpolarized light.

In elucidating the matrix element effects in the DMFT method, after writing the Lehman representation for the Greens' functions in terms of $A(\mathbf{k}, E) \rightarrow A(\varepsilon, E)$ and by using standard contour integration techniques for the $1/\beta \sum_{\omega_n}$ summation, we obtain

$$\chi^{\text{THG}}(i\nu) = -\frac{\tilde{t}^4}{3\nu^4} \int d\varepsilon D(\varepsilon) dE_1 \cdots dE_4 \quad (12)$$

$$A(\varepsilon, E_1)A(\varepsilon, E_2)A(\varepsilon, E_3)A(\varepsilon, E_4) \times F$$

with

$$F = \frac{f(E_1)}{E_1 - E_2 + i\nu} \frac{1}{E_1 - E_3 + 2i\nu} \frac{1}{E_1 - E_4 + 3i\nu} + \frac{f(E_2)}{E_2 - E_1 - i\nu} \frac{1}{E_2 - E_3 + i\nu} \frac{1}{E_2 - E_4 + 2i\nu} + \frac{f(E_3)}{E_3 - E_1 - 2i\nu} \frac{1}{E_3 - E_2 - i\nu} \frac{1}{E_3 - E_4 + i\nu} + \frac{f(E_4)}{E_4 - E_1 - 3i\nu} \frac{1}{E_4 - E_2 - 2i\nu} \frac{1}{E_4 - E_3 - i\nu}, \quad (13)$$

where f is the Fermi function. This expression closely resembles familiar expressions in nonlinear optics literature (see, e.g., Sec. 3.2 of ref. 2). Therefore, in this formulation, the matrix element effects enter via the spectral function $A(\varepsilon, E)$, which is determined only by the self-energy. In principle, after replacing $i\nu$ with $\nu + i0^+$ in this expression, we can use the spectral weights obtained from the DMFT solver to calculate the nonlinear response. However, the numerical calculation of the above 5D integrals is not computationally feasible.

Another alternative method would be to calculate χ^{THG} at Matsubara frequencies according to (11), followed by the analytic continuation $i\nu \rightarrow \nu + i0^+$. However, in this process, we face spurious features that are characteristic of the analytic continuation of numbers, which makes it difficult to assess the nonlinear dynamical structures.

Since we are interested in high energy features in the scale of the Mott gap, which is much larger than the thermal energies at room temperature, in order to avoid the above-mentioned difficulties, we work at zero temperature. At $T = 0$, (11) will be replaced by

$$\chi^{\text{THG}}(\nu) = \frac{\tilde{t}^4}{6\pi\nu^4} \int \frac{d\omega d\varepsilon D(\varepsilon)}{\xi_0 - \varepsilon} \frac{1}{\xi_1 - \varepsilon} \frac{1}{\xi_2 - \varepsilon} \frac{1}{\xi_3 - \varepsilon}, \quad (14)$$

where $\xi_j = \omega + j\nu - \Sigma_R(\omega + j\nu) + i|\Sigma_I(\omega + j\nu)|$ for $j = 0, 1, 2, 3$.

In the above formula, (i) the integration over ε corresponds to the summation over the intermediate states in conventional expressions,²⁾ which are usually used for systems with discrete energy levels, and (ii) the matrix element effects are encoded in $\Sigma(\omega)$ —real and imaginary parts of which have been denoted by Σ_R and Σ_I , respectively. *It is very crucial to note that we have used the absolute value of the imaginary part of the self-energy.* This is indeed a necessary step to shift from time-ordered four-current, to fully retarded one.³⁾

Decomposing the integrand in (14) to partial fractions

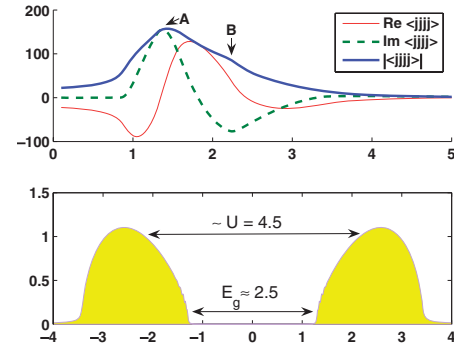


Fig. 2. THG and DOS for $U = 4.5$. We use the Bethe lattice for solving DMFT equations. In the upper panel, the dashed line is the imaginary part of $\langle JJJJ \rangle$, narrow solid line represents its real part, and the bold solid line represents its absolute value. The lower panel shows the DOS. The onset of (3-photon) absorption at $\nu \approx 0.85$ corresponds to the gap value, $E_g \approx 2.5$, while the peak-to-peak energy difference is on the scale of $U = 4.5$.

in terms of ε , the four-current correlation can be written as $f_0 + f_1 + f_2 + f_3$, where

$$f_j(\nu) = \frac{\tilde{t}^4}{6\pi} \int d\omega \prod_{s \neq j} \frac{1}{\xi_j - \xi_s} \int d\varepsilon \frac{D(\varepsilon)}{\varepsilon - \xi_j}. \quad (15)$$

Equation (15) reveals the resonance structure transparently: It arises from $\omega + j\nu - \Sigma_R(\omega + j\nu) = \varepsilon$. When the frequency ν of the photons is such that the j -photon frequency matches the energy difference $\varepsilon - \omega + \Sigma_R(\omega + j\nu)$, we will have a j -photon resonance. Here, f_0 corresponds to a background contribution.

Note that we do not have any control over the “broadening” parameter η within this formulation, instead the broadening $\eta = |\Sigma_I(\omega)|$ is determined by the solution of the impurity problem in a self-consistent fashion.

Now, let us present our results. For a semicircular Bethe lattice DOS of width $2\tilde{t} = 1$, the critical value is given by $U_c \approx 3.3$, above which the system is in the Mott insulating state. Figure 2 shows the result for $U = 4.5$. The lower panel shows the self-consistent DOS with a Mott-Hubbard gap ~ 2.5 . The peak-to-peak separation between the upper and lower Hubbard bands is approximately $U = 4.5$. The upper panel shows the real part (dashed), imaginary part (dotted), and absolute value (solid line) of the four-current correlation $\langle JJJJ \rangle^{\text{THG}}$.

The onset of absorption starts at $\nu \approx 0.85$, which is $1/3$ the gap magnitude. This can be clearly seen in the imaginary part of the THG four-current correlation in Fig. 2. This onset clearly corresponds to the three-photon absorption. The three-photon resonance peaks are observed at around $\nu \approx 1.5$ (denoted by A), which is $1/3$ the peak-to-peak separation of the Hubbard bands. Further, the weaker feature (denoted by B), which is a shoulder similar to the finite-dimensional results,⁵⁾ corresponds to $1/2$ peak-to-peak separation (~ 4.5) of the Hubbard bands. The one-photon process is the weakest feature around $\nu \sim 4.5$, which can hardly be distinguished in the THG spectrum. However, although the DMFT is designed to work better in larger dimensions, the spectrum in Fig. 2 qualitatively resembles the experimental result of Sr_2CuO_3 , which is a one-dimensional Mott insulator.⁵⁾

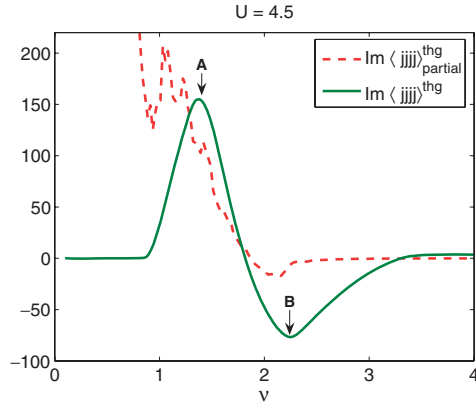


Fig. 3. Solid line shows the imaginary part of the total THG for $U = 4.5$. The dashed line shows the imaginary part of $f_3(v)$. The points **A** and **B** in this figure correspond to those in Fig. 2.

We claimed that in peak **A** of Fig. 2, the dominant contribution comes from the three-photon processes. To demonstrate this, we plot the imaginary part of $f_3(v)$ with dashed line in Fig. 3. The solid line shows the total four-current correlation. As can be seen, the three-photon resonance dominantly contributes to peak **A**, although it is slightly shifted to lower energies. Further, it is clearly seen that $f_3(v)$ does not contribute significantly to the two-photon resonance at **B**. $f_3(v)$ also blows up at small frequencies, which according to (15) will be finally compensated by other partial spectra f_0, f_1, f_2 , to give the total THG spectrum.

In Fig. 4, we plot $\text{Im } f_3(v)/E_g$ for Mott insulators with various values of U as a function of v/E_g . We also apply an overall scaling to the curves. Such a scaling behavior, though approximate, points to a universal features in the nonlinear optical spectra of the Mott insulators, which are independent of the gap magnitude. It seems that the mean field scaling behavior³⁾ survives the quantum fluctuations implemented by DMFT. It would be interesting to further explore this observation by using alternative methods of dealing with correlated insulators.

In summary, on the technical side, we have formulated the nonlinear optical response theory within the DMFT theory. In eq. (14), we present a feasible solution for avoiding numerical difficulties. From the physics viewpoint, assuming that DMFT is a good approximation for $d > 1$, we observe that the nonlinear optical spectra of higher dimensional Mott insulators share common features with those observed in the $d = 1$ dimensional Mott insulator Sr_2CuO_3 .⁵⁾ Further, within the DMFT, we observe an approximate scaling behavior in the THG spectra of Mott insulators.

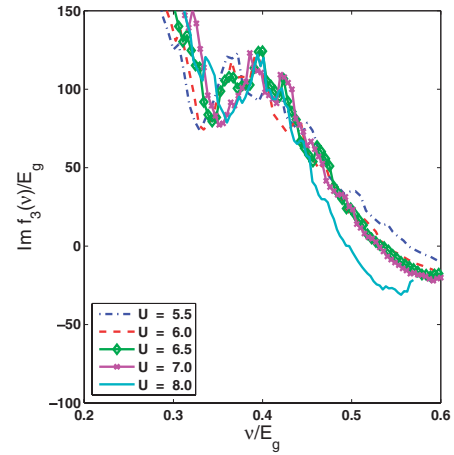


Fig. 4. Imaginary part of $f_3(v)/E_g$ vs v/E_g , where E_g is the Mott–Hubbard gap in the Mott insulating phase.

Acknowledgment

S.A.J. was supported by JSPS fellowship P04310. We wish to thank M. J. Rozenberg for allowing the use of his code in solving the DMFT equations. This work was supported by a Grant-in-Aid for Scientific Research from the Ministry of Education, Culture, Sports, Science and Technology and by the NAREGI project.

- 1) S. Mukamel: *Principles of Nonlinear Optical Spectroscopy* (Oxford University Press, 1995).
- 2) R. W. Boyd: *Nonlinear Optics* (Academic Press, 2003) 2nd ed.
- 3) S. A. Jafari, T. Tohyama and S. Maekawa: J. Phys. Soc. Jpn. **75** (2006) 054703.
- 4) H. Kishida, H. Matsuzaki, H. Okamoto, T. Manabe, M. Yamashita, Y. Taguchi, Y. Tokura: Nature **405** (2000) 929, and references therein.
- 5) H. Kishida, M. Ono, K. Miura, H. Okamoto, M. Izumi, T. Manako, M. Kawasaki, Y. Taguchi, Y. Tokura, T. Tohyama, K. Tsutsui and S. Maekawa: Phys. Rev. Lett. **87** (2001) 177401.
- 6) Y. Mizuno, K. Tsutsui, T. Tohyama and S. Maekawa: Phys. Rev. B **62** (2000) R4769.
- 7) T. Tohyama and S. Maekawa: J. Lumin. **94–95** (2001) 659.
- 8) A. Georges, G. Kotliar, W. Krauth and M. J. Rozenberg: Rev. Mod. Phys. **68** (1996) 13.
- 9) X. Y. Zhang, M. J. Rozenberg and G. Kotliar: Phys. Rev. Lett. **70** (1993) 1666.
- 10) We use the code distributed by M. J. Rozenberg to participants in the summer 2002 Trieste workshop on strongly correlated electron systems.
- 11) W. Wu: Phys. Rev. Lett. **61** (1988) 1119.
- 12) K. Chuo, Z. Su, B. Hao and L. Yu: Phys. Rep. **118** (1985) 1.
- 13) J. Yu and W. P. Su: Phys. Rev. B **44** (1991) 13315.
- 14) M. E. Peskin and D. V. Schroeder: *An Introduction to Quantum Field Theory* (Westview Press, 1995).